

Ultra-Compact Subwavelength-Grating-Assisted Polarization-Independent Directional Coupler

Heng Xie, Jiajiu Zheng^{id}, Peipeng Xu^{id}, Jianting Yao, James Whitehead, and Arka Majumdar

Abstract—We propose and experimentally demonstrate an ultra-compact, low-loss polarization-independent directional coupler on the silicon-on-insulator (SOI) platform. By exploiting subwavelength gratings in the directional coupler, the coupling strength could be made equal for both transverse-electric and transverse-magnetic polarizations. The demonstrated polarization-independent directional coupler has a device length of only 4.5 μm and achieves complete cross-coupling with a low excess loss of <1 dB over a bandwidth of ~ 65 nm. The reported devices also demonstrate robust fabrication tolerance.

Index Terms—Integrated optics, couplers, subwavelength structures.

I. INTRODUCTION

THE silicon-on-insulator (SOI) based photonic components have generated strong interest in recent years due to its compactness, compatibility with the mature CMOS fabrication processes, resulting in low manufacturing costs, and the potential to create large-scale photonic integrated circuits (PICs) [1]. The SOI waveguides provide a very high index contrast between silicon ($n \sim 3.46$) and its cladding, silicon dioxide ($n \sim 1.45$), enabling a strong confinement of light with sub-micron cross sections. However, the enhanced index contrast also imposes a high birefringence in an asymmetric SOI waveguide, and the integrated silicon photonic devices are generally polarization dependent [2]. A directional coupler (DC) is one of the most important components in the PICs because it performs the functions of beam splitting and combining. Owing to their simplicity and ease of design, DCs have been widely used to construct

optical switches [3], [4], optical power splitter [5]–[7], and polarization-controlling devices [8], [9]. However, for silicon photonic DCs, the coupling length for transverse-electric (TE) mode differs from that for transverse-magnetic (TM) mode, and these DCs are usually polarization-sensitive and can work for only one specific polarization.

To overcome this issue, two separate circuits consisting of polarization splitters and rotators are used for two orthogonal polarizations [10]. In this way, polarization-independent operation can be achieved, albeit at the expense of increased system size and complexity. A more straightforward solution is to realize the inherently polarization-independent devices. Many structures have been proposed to implement the polarization-independent DC, including slot waveguides, bent waveguides and subwavelength gratings. Slot waveguides can eliminate the polarization dependence in DCs but result in a high propagation loss owing to the scattering in the slot and relatively complicated circuits because of the requirement of strip-slot converters [11]. DCs consisting of two cascaded bent waveguides are also utilized to realize polarization-independent power splitters [12]. The major disadvantage of such a structure is the quite large device size since each bent region works only for one polarization. Subwavelength gratings (SWGs) provide the flexibility to engineer the index profiles and have also been used in various DCs [13], [14]. By adjusting the duty cycle of SWGs, polarization-independent directional couplers based on both slot waveguides with subwavelength gratings has been demonstrated [15]. Recently, a polarization-independent DC utilizing nonuniform “nano-teeth” in the coupling region is proposed to function as both complete coupler and 3-dB splitter [16]. The device possesses a compact footprint, but suffers from a quite small feature size, which is challenging in term of fabrication reproducibility and tolerance.

In this Letter, we propose and demonstrate an ultra-compact polarization-independent DC by utilizing subwavelength gratings in strip waveguides. As compared to the conventional DC, the SWG structure in silicon makes the coupling strength equal for both TE and TM polarizations. Benefiting from this design, polarization independent DC with broadband operation (1500–1565 nm) exceeding the entire C-band is demonstrated both numerically and experimentally with the beat length of only $\sim 4.5 \mu\text{m}$.

II. STRUCTURE AND DESIGN

For the conventional DCs consisting of silicon waveguides, the coupling strength for TM polarization is much higher than

Manuscript received March 13, 2019; revised August 23, 2019; accepted August 25, 2019. Date of publication August 27, 2019; date of current version September 4, 2019. This work was supported in part by the National Natural Science Foundation of China under Grant 61875099 and Grant 61505092, in part by the Natural Science Foundation of Zhejiang Province under Grant LY18F050005, in part by the Air Force Office of Scientific Research (AFOSR) under Grant FA9550-17-C-0017, and in part by the K. C. Wong Magna Fund at Ningbo University. (Corresponding author: Peipeng Xu.)

H. Xie, P. Xu, and J. Yao are with the Laboratory of Infrared Materials and Devices, Advanced Technology Research Institute, Ningbo University, Ningbo 315211, China, and also with the Key Laboratory of Photoelectric Detection Materials and Devices of Zhejiang Province, Ningbo 315211, China (e-mail: 1280112208@qq.com; xupeipeng@nbu.edu.cn; 529600365@qq.com).

J. Zheng and J. Whitehead are with the Department of Electrical Engineering, University of Washington, Seattle, WA 98195 USA (e-mail: jjzno1@gmail.com; jamesw25@uw.edu).

A. Majumdar is with the Department of Electrical Engineering, University of Washington, Seattle, WA 98195 USA, and also with the Department of Physics, University of Washington, Seattle, WA 98195 USA (e-mail: arka@uw.edu).

Color versions of one or more of the figures in this letter are available online at <http://ieeexplore.ieee.org>.

Digital Object Identifier 10.1109/LPT.2019.2937890

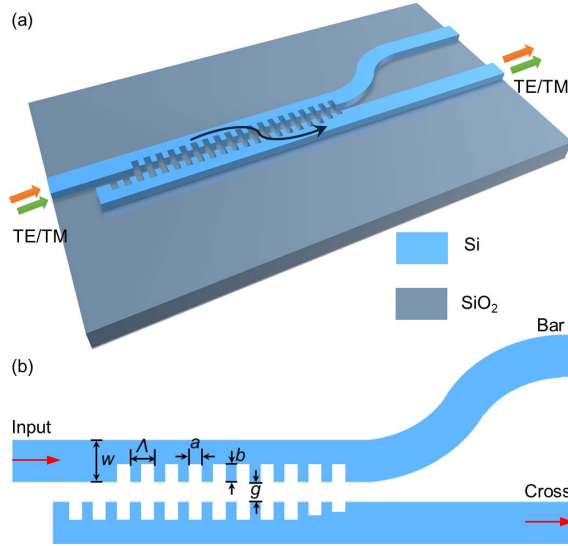


Fig. 1. Schematic of the SWG polarization-independent DC; (a) 3D perspective view and (b) top view with the designed parameters labeled.

that for TE polarization. To obtain a polarization-independent DC, SWG waveguides are utilized to enhance the coupling strength for TE polarization while maintaining the coupling strength for TM polarization, making it possible to obtain equal coupling strengths for both TE and TM polarizations.

Figure 1(a) shows the schematic of the polarization-independent DCs based on the SWG structure. It consists of two parallel silicon strip waveguides with two arrays of SWGs placed in the inner sidewalls in the coupling region. By engineering the SWGs, the light propagating in the SWGs can be considered as if it is propagating in an equivalent strip waveguide with an effective refractive index. From the top view of the polarization-independent DC, shown in Fig. 1(b), the length of low and high refractive segment, namely, groove and ridge are a and $\Lambda - a$, respectively and the depth of grating pitch is b . The waveguide width W is chosen to be 360 nm to satisfy the single-mode condition and ensure efficient coupling. To circumvent the Bragg diffraction due to the larger values of the period, Λ is chosen to meet $\Lambda < \lambda / (2n_{\text{SWG,eff}})$, where λ is 1550 nm and $n_{\text{SWG,eff}}$ represents the effective index of the fundamental Bloch mode in the two SWG waveguides. Since the $n_{\text{SWG,eff}} < 2.3$ in all cases, we choose $\Lambda = 210$ nm. Considering the ease of the fabrication, the fill factor (defined as the ratio of a to Λ) should be ~ 0.5 and the groove width of a and grating depth b are set to be 90 nm and 100 nm, respectively. An S-bend with a radius of $5 \mu\text{m}$ is used near the output ports to decouple the waveguides. The refractive indices of silicon and silicon dioxide used in the simulations are $n_{\text{Si}} = 3.455$ and $n_{\text{SiO}_2} = 1.445$, respectively. We used PMMA as the upper cladding for the ease of device fabrication. However, using SiO_2 as the cladding material, which is often used in silicon photonics, does not change the performance of the device.

When light propagates in a conventional DC, the guiding behavior can be described by the mode interference between the two supermodes in coupled-waveguide system. Here, the fundamental mode is the even supermode and the first

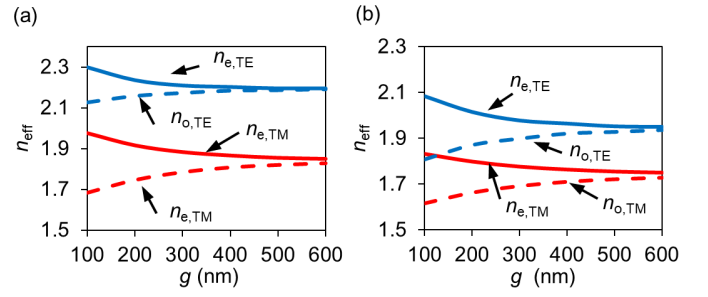


Fig. 2. Effective indices of even and odd TE modes ($n_{e,\text{TE}}$, $n_{o,\text{TE}}$) and TM modes ($n_{e,\text{TM}}$, $n_{o,\text{TM}}$) in (a) conventional DC and (b) SWGs DC as a function of the coupling gap g .

higher order mode is the odd supermode. The beat length L_π of these two modes can be determined by

$$L_\pi = \frac{\pi}{\beta_{\text{even}} - \beta_{\text{odd}}} = \frac{\lambda}{2(n_{\text{even}} - n_{\text{odd}})}$$

where n_{even} and n_{odd} are the effective indices of the two modes, respectively. For our proposed SWG DCs, three-dimensional finite-difference time-domain (3D FDTD)-based band structure calculations were performed using Lumerical Solutions to obtain the effective indices of the excited Bloch mode. Only one period of the SWG was simulated and Bloch boundary conditions were used in the direction of mode propagation.

Figure 2(a) shows the effective index of the even and odd modes for conventional DCs with 360-nm width for both TE ($n_{e,\text{TE}}$ and $n_{o,\text{TE}}$) and TM ($n_{e,\text{TM}}$ and $n_{o,\text{TM}}$) polarizations, which are calculated by an eigenmode solver (Lumerical Mode Solutions) at the wavelength of 1550 nm. We find that the refractive index difference between the even and odd mode for TM polarization is always greater than that for TE polarization with any coupling gap g and hence, it is difficult to achieve polarization-independent DCs with silicon photonic strip waveguides. Compared to the conventional DC, with the SWG structure into the inner sidewalls, the effective indices $n_{e,\text{TE}}$ and $n_{o,\text{TE}}$ for TE polarization present a dramatic change due to the strong field distribution near the inner sidewalls. Specifically, the index perturbation for the even mode is moderate due to the symmetric field profile in the coupling region while the index perturbation for the odd mode is strongly altered in the central region because the odd mode has an anti-symmetric field profile. Thus, the effective index difference between the even and odd modes for TE polarization are enlarged. For TM polarization, the electric field is mainly distributed in the upper and lower surfaces, and the perturbation induced by the SWG structure changes the effective index by a small amount. Therefore, the refractive index difference between even and odd modes for both polarizations can be identical when adjusting the coupling gap. Considering the trade-off between the coupling efficiency and ease of fabrication, the coupling gap g is chosen to 180 nm. The coupling length for two polarizations is $\sim 4.5 \mu\text{m}$, indicating an ultra-compact polarization-independent DC can be achieved.

Figures 3(a) and 3(b) show the simulated light propagation in the designed polarization-independent DC at the

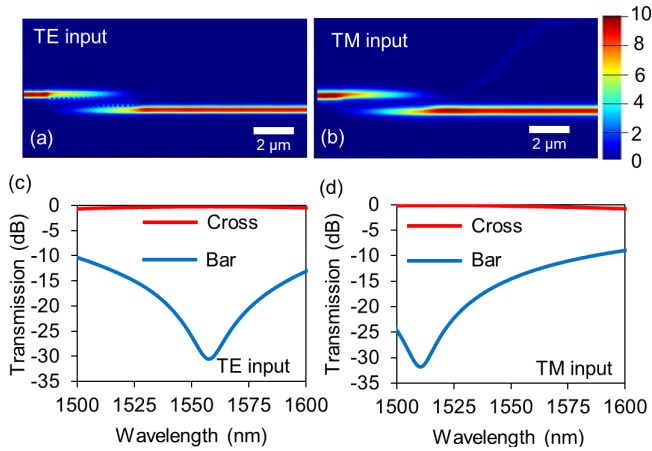


Fig. 3. The intensity along the device when (a) TE and (b) TM polarizations are launched. (c), (d) Calculated transmission at the cross and bar ports for (c) TE and (d) TM modes.

wavelength of 1550 nm when TE and TM polarization modes are launched from the input ports. A complete cross-coupling can be observed for both polarizations. We also find that the evanescent coupling for TE polarization is dramatically enhanced, while the evanescent coupling enhancement is quite weak in the gap region for TM polarization, making the coupling strengths for TE and TM polarizations identical. Figures 3(c) and 3(d) show the calculated transmission spectrum of the device for both polarizations over the wavelength from 1500 nm to 1600 nm. Across the whole wavelength band, the present polarization-independent DC attains the coupling losses of <0.8 dB for both polarizations. Moreover, the polarization dependence losses (PDLs, defined as the ratio of the transmittances at the Cross port between TE and TM polarizations) are calculated to be ~ 0.4 dB. The extinction ratios (ERs, defined as the contrast ratio between the two output ports) of $> \sim 10$ dB are achieved for both polarization modes between two output ports across the whole wavelength range.

III. FABRICATION AND CHARACTERIZATION

The designed polarization-independent DCs were fabricated using SOI wafers with a 250-nm-thick silicon layer on top of a 3-μm-thick buried oxide layer. The pattern was defined by a JEOL JBX-6300FS 100kV electron-beam lithography (EBL) system using positive tone ZEP-520A resist and transferred to the silicon layer by inductively coupled plasma (ICP) etcher utilizing a gas mixture of SF₆ and C₄F₈. Finally, the whole device was covered with a 300-nm thick PMMA layer as the top cladding. To characterize the performance for both TE and TM polarizations, appropriately designed grating couplers (GCs) for TE and TM polarizations were used [17], as shown in Figs. 4(a)-4(b). The strip waveguides with TE or TM-type grating couplers were also fabricated on the same chip for normalization. Figures 4(c)-4(d) show the scanning electron micrographs (SEM) of the device and the enlarged view of the coupling region. Figures 4(e) and 4(f) show the fully etched TE-type and TM-type focusing sub-wavelength GCs [17]. We probed the devices using an optical

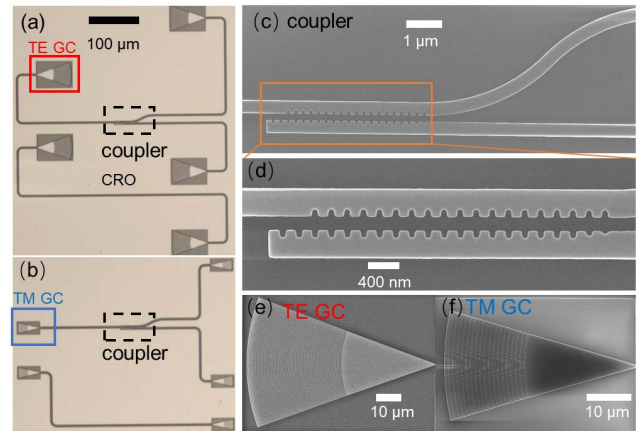


Fig. 4. (a), (b) Optical microscope image of the fabricated polarization-independent DCs. (c), (d) SEM of the device and the enlarged view of the coupling region. (e), (f) SEMs of the GCs.

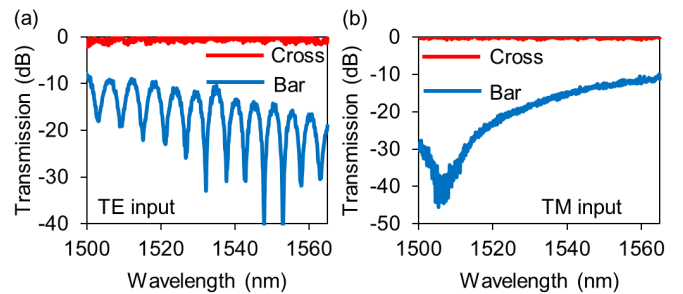


Fig. 5. Measured spectral responses of the fabricated polarization-independent DCs for (a) TE input and (b) TM input.

fiber setup. The polarization of the input light was controlled to match the fundamental quasi-TE/TM mode of the waveguide by a manual fiber polarization controller (Thorlabs FPC526). A tunable continuous wave laser (Santec TSL-510) and a low-noise power meter (Keysight 81634B) were used to measure the performance of the fabricated devices.

Figures 5(a) and 5(b) show the measured transmission spectrum for TE and TM polarizations in the wavelength range 1500 to 1565 nm. The upper bound of the wavelength measurement range is limited by our tunable laser. The cross-coupling loss is <1 dB for both polarizations across the whole wavelength range. The measured coupling loss for TE polarization is a little bit higher than the simulation results. This mismatch is primarily due to the relatively high scattering loss induced by sidewall roughness. The ER for TE mode was almost greater than 10 dB over the whole wavelength range. Some ripples are observed in bar port, which is due to the reflection of both end facets of the input waveguide. For the TM polarization, the measured excess loss is <0.4 dB, which is comparable with the simulation results since the transmission of TM mode is less sensitive to sidewall roughness. The ER is >10 dB with a maximum value of ~ 46 dB, which is larger than the simulated one. This can be attributed to the more complete cross-coupling for TM polarization due to the slight fabrication deviation. We note that the performance of the polarization-independent DCs could be further improved by optimizing the fabrication processes.

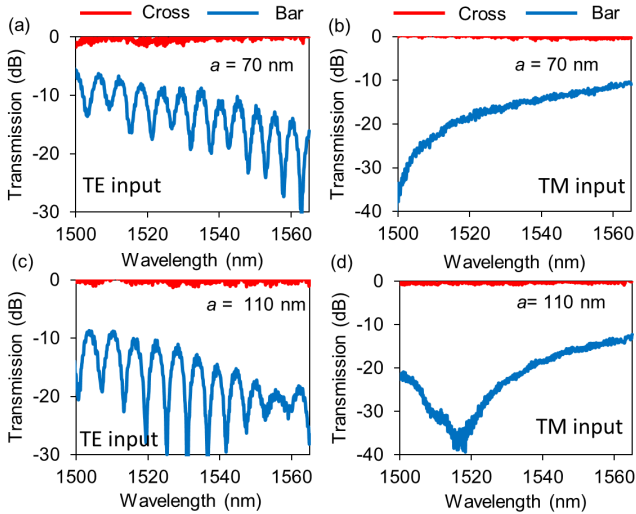


Fig. 6. Measurement results for the polarization-independent DCs with groove width variations: (a) TE polarization when $a = 70$ nm, (b) TM polarization when $a = 70$ nm, (c) TE polarization when $a = 110$ nm, and (d) TM polarization when $a = 110$ nm.

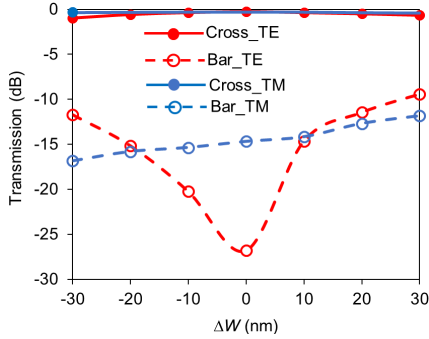


Fig. 7. Fabrication tolerance of the designed polarization-independent DCs with variation ΔW .

To check the fabrication tolerance of the present polarization-independent DCs, we also fabricated the devices with different groove widths on the same chip, i.e., $a = 70$ nm, and $a = 110$ nm. The measured spectra are shown in Figs. 6(a)-(d). The excess loss and the ER do not change significantly even when the change of groove width varies from -20 nm to $+20$ nm, and the ER is roughly higher than 10 dB over a bandwidth of ~ 50 nm, except for the case with $a = 70$ nm with short wavelength TE polarization input. Such a good fabrication tolerance ± 20 nm is well within the capabilities of current fabrication technologies.

The fabrication tolerance of the designed polarization-independence directional coupler (DC) is further analyzed. The variations in the x and y dimensions is denoted by ΔW . The transmission at the center wavelength of 1550 nm as a function of the waveguide width variation ΔW ($W = W + \Delta W$, $g = g - \Delta W$, $a = a - \Delta W$) are shown in Fig. 7. The present device maintains a coupling loss lower than 1 dB (0.4 dB) for TE (TM) as well as a good ER (> 10 dB) with the fabrication error of $(-30, 30)$ nm.

IV. CONCLUSION

We designed and experimentally demonstrated ultra-compact polarization-independent DCs using SWGs. The SWG structure is designed to enhance the evanescent coupling of TE modes so that the beat length for both TE and TM can be identical. The measurement results show a low excess loss ($< \sim 1$ dB) and PDLs ($< \sim 0.4$ dB). Functioning as 50/50 power splitter, 3-dB coupler can be used to construct the Mach-Zehnder switches/modulators. In order to realize polarization-insensitive operation, it is highly desirable to develop a polarization-insensitive 3-dB coupler, which can be easily achieved by adjusting the coupling strength of the uniform subwavelength structure. The availability of such compact, low loss and polarization-independent DCs will find numerous applications in on-chip photonic integrated circuits.

REFERENCES

- [1] R. Soref, "The past, present, and future of silicon photonics," *IEEE J. Sel. Topics Quantum Electron.*, vol. 12, no. 6, pp. 1678–1687, 2006.
- [2] D. Dai, L. Liu, S. Gao, D.-X. Xu, and S. He, "Polarization management for silicon photonic integrated circuits," *Laser Photon. Rev.*, vol. 7, no. 3, pp. 303–328, 2013.
- [3] J. V. Campenhout, W. M. J. Green, S. Assefa, and Y. A. Vlasov, "Low-power, 2×2 silicon electro-optic switch with 110-nm bandwidth for broadband reconfigurable optical networks," *Opt. Express*, vol. 17, no. 26, pp. 24020–24029, Dec. 2009.
- [4] S. Chen, Y. Shi, S. He, and D. Dai, "Low-loss and broadband 2×2 silicon thermo-optic Mach-Zehnder switch with bent directional couplers," *Opt. Lett.*, vol. 41, no. 4, pp. 836–839, Feb. 2016.
- [5] H. Yun *et al.*, "Broadband 2×2 adiabatic 3 dB coupler using silicon-on-insulator sub-wavelength grating waveguides," *Opt. Lett.*, vol. 41, no. 13, pp. 3041–3044, Jun. 2016.
- [6] Y. Wang *et al.*, "Compact broadband directional couplers using sub-wavelength gratings," *IEEE Photon. J.*, vol. 8, no. 3, Jun. 2016, Art. no. 7101408.
- [7] R. Halir *et al.*, "Colorless directional coupler with dispersion engineered sub-wavelength structure," *Opt. Express*, vol. 20, no. 12, pp. 13470–13477, Jun. 2012.
- [8] D. Dai, Z. Wang, and J. E. Bowers, "Ultrashort broadband polarization beam splitter based on an asymmetrical directional coupler," *Opt. Lett.*, vol. 36, no. 13, pp. 2590–2592, 2011.
- [9] Y. Song and P. Xu, "Design of ultra-low insertion loss active transverse electric-pass polarizer based $\text{Ge}_2\text{Sb}_2\text{Te}_5$ on silicon waveguide," *Opt. Commun.*, vol. 426, pp. 30–34, Nov. 2018.
- [10] T. Barwicz *et al.*, "Polarization-transparent microphotonic devices in the strong confinement limit," *Nature Photon.*, vol. 1, no. 1, pp. 57–60, 2007.
- [11] T. Fujisawa and M. Koshiba, "Polarization-independent optical directional coupler based on slot waveguides," *Opt. Lett.*, vol. 31, pp. 56–58, Jan. 2006.
- [12] X. Chen, W. Liu, Y. Zhang, and Y. Shi, "Polarization-insensitive broadband 2×2 3 dB power splitter based on silicon-bent directional couplers," *Opt. Lett.*, vol. 42, no. 19, pp. 3738–3740, Sep. 2017.
- [13] P. Cheben, R. Halir, J. H. Schmid, H. A. Atwater, and D. R. Smith, "Subwavelength integrated photonics," *Nature*, vol. 560, pp. 565–572, Aug. 2018.
- [14] R. Halir *et al.*, "Waveguide sub-wavelength structures: A review of principles and applications," *Laser Photon. Rev.*, vol. 9, no. 1, pp. 25–49, 2015.
- [15] L. Liu, Q. Deng, and Z. Zhou, "Subwavelength-grating-assisted broadband polarization-independent directional coupler," *Opt. Lett.*, vol. 41, no. 7, pp. 1648–1651, Apr. 2016.
- [16] H. Xu and Y. Shi, "Ultra-compact polarization-independent directional couplers utilizing a subwavelength structure," *Opt. Lett.*, vol. 42, no. 24, pp. 5202–5205, Dec. 2017.
- [17] Y. Wang *et al.*, "Focusing sub-wavelength grating couplers with low back reflections for rapid prototyping of silicon photonic circuits," *Opt. Exp.*, vol. 22, no. 17, pp. 20652–20662, 2014.